

## Local tuning of photonic crystal cavities using chalcogenide glasses

Andrei Faraon,<sup>1,a)</sup> Dirk Englund,<sup>1</sup> Douglas Bulla,<sup>2</sup> Barry Luther-Davies,<sup>2</sup> Benjamin J. Eggleton,<sup>3</sup> Nick Stoltz,<sup>4</sup> Pierre Petroff,<sup>4</sup> and Jelena Vučković<sup>5</sup>

<sup>1</sup>Department of Applied Physics, Stanford University, Stanford, California 94305, USA

<sup>2</sup>Centre for Ultrahigh-bandwidth Devices for Optical Systems (CUDOS), Laser Physics Centre, Australian National University, Canberra, ACT 0200, Australia

<sup>3</sup>Centre for Ultrahigh-bandwidth Devices for Optical Systems (CUDOS), School of Physics, University of Sydney, Sydney, NSW, 2006, Australia

<sup>4</sup>Department of Electrical and Computer Engineering, University of California, Santa Barbara, California 93106, USA

<sup>5</sup>E. L. Ginzton Laboratory, Stanford University, Stanford, California 94305, USA

(Received 5 November 2007; accepted 8 January 2008; published online 31 January 2008)

We demonstrate a method to locally change the refractive index in planar optical devices by photodarkening of a thin chalcogenide glass layer deposited on top of the device. The method is used to tune the resonance of GaAs-based photonic crystal cavities by up to 3 nm at 940 nm. The method has broad applications for postproduction tuning of photonic devices. © 2008 American Institute of Physics. [DOI: 10.1063/1.2839308]

On-chip integration of optical components promises to greatly enhance speed and reduce costs in optical communication applications, such as interconnects and optical logic. Photonic crystal (PC) devices are one of the most promising platforms for on-chip integration, as they can combine optical waveguides, resonators, dispersive devices, lasers, or modulators.<sup>1–4</sup> Such devices can be patterned with existing semiconductor lithographic techniques. However, they are highly sensitive to fabrication imperfections<sup>5</sup> and a practical method to locally tune their optical properties is needed. In this paper, we present a method for tuning GaAs PC devices based on chalcogenide glasses. Chalcogenide glasses change their optical properties when illuminated with light above their band gap and have been used to tune optical devices as quantum cascade lasers.<sup>6</sup> The tuning of PC devices directly fabricated in chalcogenide glasses has already been shown in Ref. 7 but many other applications rely on PC fabricated in other materials such as group IV and III-V semiconductors. One such application is quantum information with InAs quantum dots (QDs) embedded in GaAs photonic crystal structures.<sup>8–10</sup> The performance of these devices relies on precise wavelength matching of the cavity to embedded QDs. One way to achieve spectral matching is by temperature tuning, which shifts the cavity and QD at different rates so that they can be made to intersect if the original mismatch is small.<sup>9</sup> However, it is often necessary to shift the cavity independently as well, especially in photonic networks.<sup>10</sup> To date, several nonlocal techniques have been developed to control cavity wavelength (see Refs. 11 and 12) and a local tuning method based on tuning the resonance by bringing a nanowire in the proximity of the photonic crystal cavity has been reported by Grillet *et al.* in Ref. 13. However, none of these techniques is reliable for independent on-chip tuning of large ensembles of photonic crystal cavities.

In our approach, a photosensitive chalcogenide glass layer is deposited on prefabricated GaAs/InAs devices. Linear three-hole defect<sup>14</sup> PC cavities were first fabricated in a 150 nm thick GaAs membrane containing a central layer of

InAs QDs, as described in Ref. 15. Arsenic trisulphide films with thickness between 30 and 100 nm were deposited onto the photonic crystals using thermal evaporation from a temperature controlled baffled boat in a chamber pumped to a base pressure of  $3 \times 10^{-7}$  torr. The deposition geometry was chosen to ensure that the flux of material struck the sample close to normal incidence to prevent coating the inside of the holes. To improve film adhesion, the sample surfaces were cleaned using 50 eV Ar ions prior to deposition.

Thermal evaporation results in films with substantially different bond structure from the bulk glass. The films have been found to contain disconnected molecular cagelike structures<sup>16</sup> that form in the vapor phase and are then frozen into the deposited film. These cagelike structures are, however, metastable and can “open” with optical excitation near the band edge or by heating that allows rebonding to occur which results in polymerization of a more extended glass network. This rebonding process is accompanied by an increase in the refractive index and a small decrease of the material volume.<sup>17</sup> This change is permanent unless the glass is annealed above the glass transition temperature which can potentially reset the initial refractive index.<sup>6</sup> The thermally evaporated films had an index (at 1550 nm) of  $\sim 2.31$  compared with the bulk glass whose index is 2.43. After deposition, the films were partially polymerized by annealing at 130 °C for 24 h prior to use, which increased the refractive index to  $\sim 2.38$ . Subsequent irradiation of the films with actinic light at high fluence can increase the film index to the bulk value.

The experiment was performed at cryogenic temperature (less than  $\sim 60$  K) to obtain luminescence from the embedded InAs quantum dots, as needed for quantum information processing applications. This illustrates that the method works at low temperatures, though we stress that it is applicable to room temperature nanophotonic circuits. The sample was placed inside a continuous-flow liquid helium cryostat at 10 K and the QD photoluminescence was used to measure the cavity resonance. A confocal microscope setup and a laser tuned at 780 nm excited quantum dot luminescence while a spectrometer monitored the signal. A 543 nm HeNe laser (1  $\mu$ W) focused to  $\sim 1 \mu\text{m}^2$  through the same confocal setup

<sup>a)</sup>Electronic mail: faraon@stanford.edu.

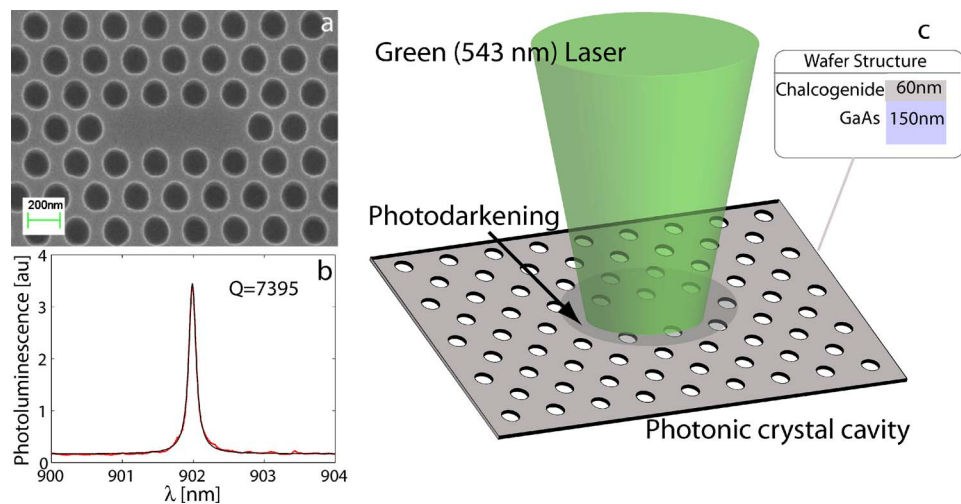


FIG. 1. (Color online) (a) Scanning electron microscope image of the photonic crystal cavity fabricated in GaAs before the deposition of  $\text{As}_2\text{S}_3$ . (b) Cavity spectrum before the chalcogenide deposition indicating a quality factor  $Q=7395$ . (c) Schematic of the method for local cavity tuning. A layer of  $\text{As}_2\text{S}_3$  is deposited on top of the photonic crystal cavity. Then, a laser tuned close to the  $\text{As}_2\text{S}_3$  band gap is focused on the cavity, increasing the effective refractive index and causing a resonance redshift.

was used for photodarkening of the  $\text{As}_2\text{S}_3$  layer (Fig. 1). This wavelength was chosen because it is close to the 527 nm bandgap of  $\text{As}_2\text{S}_3$ .

The thickness of the  $\text{As}_2\text{S}_3$  influences both the quality factor of the cavity and the maximum tuning range. For this reason, we experimented with three different thicknesses: 30, 60, and 100 nm (samples *S30*, *S60*, and *S100*). For each sample, the spectrum of the cavities was recorded before and after the deposition of the chalcogenide layer. For sample *S60* (*S30*), the deposition caused the quality factor to degrade by  $\sim 5\%$  (30%) from an average value of  $\sim 8500$  (10 000) while the resonant wavelength shifted by  $\sim 40$  nm (28 nm). The starting values for  $Q$  are different because of fluctuations in the fabrication process. Even though the starting value for  $Q$  is different for *S30* and *S60*, after the deposition,  $Q$  drops to a similar value for both samples ( $\sim 8000$  and  $\sim 7000$ ). We think that after the deposition,  $Q$  becomes limited by surface roughness of the glass layer. For sample *S100*, the  $Q$  degradation was more severe, from  $\sim 6500$  to  $\sim 1000$ , and for this reason we mainly concentrate on samples *S30* and *S60*.

With the chips mounted in the cryostat, we focused the 543 nm laser on the PC cavities for a fixed time and recorded the cavity spectrum. For sample *S60*, the cavity resonance shifted by up to 3 nm, as shown in Fig. 2(a). For 1  $\mu\text{W}$  of green laser power focused on a spot size of  $\sim 1 \mu\text{m}^2$ , the

cavity tuning rate levels off after about 20 min, as shown in Fig. 2(b). We observed that this saturation time decreases with increasing power of the 543 nm laser. During the tuning process,  $Q$  degraded to 4650. The maximum tuning range depends on the thickness of the chalcogenide layer. For 30 and 100 nm, tunings of 1 nm [Fig. 2(b)] and 4 nm were observed, respectively. Similar to *S60*, the quality factor for *S30* also degraded to  $Q \sim 4650$ . We suspect that this is a limiting value given by a loss mechanism in the glass layer. It is possible that during the tuning process, there are dislocations in between the glass layer and the GaAs substrate which induce scattering loss. The change of the cavity resonance was stable after the green laser was turned off.

Illumination of  $\text{As}_2\text{S}_3$  with light at 543 nm causes changes both in the refractive index and in the density of the material. Experiments at room temperature with films of  $\text{As}_2\text{S}_3$  show that the increase in the refractive index is accompanied by a  $\sim 1.5\%$  decrease in the film thickness. The decrease in thickness should result in a blueshift of the cavity resonance. The redshift observed experimentally implies that the dominant effect responsible for the shift of the cavity resonance is the change in the refractive index.

The behavior of the QDs during the tuning process is important for applications where QDs need to be spectrally aligned. In Fig. 3, we show the tuning of a cavity that has several QD lines weakly coupled to it. For this data set, we used a sample with 50 nm of  $\text{As}_2\text{S}_3$ . Early in the exposure, these lines shift in the characteristic fashion shown in Fig. 3: QDs first rapidly redshift then relax to a constant frequency. As coupled QDs tune across the cavity spectrum, they become bright due to the enhanced emission rate and outcoupling efficiency.<sup>15</sup> The cavity itself steadily redshifts even after the QDs have stopped tuning. We attribute the QD tuning behavior to strain in the sample. Initially, strain builds up as the sample is cooled to  $\sim 10$  K because its thermal expansion coefficients are larger than that of GaAs.<sup>18</sup> The strain increases as the tuning beam is applied and the chalcogenide compresses, reaching a maximum after about 36 s in Fig. 3. About 1 min into exposure, the strain appears to relax as the QDs settle to a fixed emission wavelength. We attribute the relaxation to nanofracturing of the chalcogenide glass as

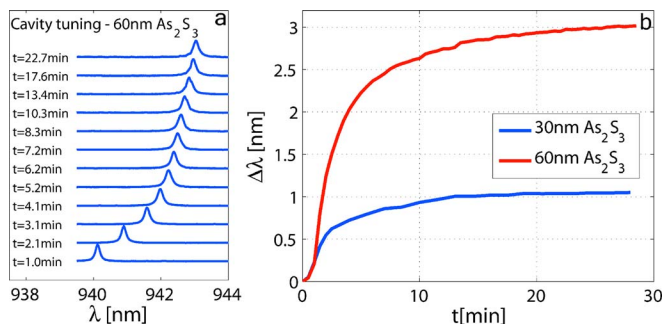


FIG. 2. (Color online) (a) Spectra showing the shift of the cavity resonance because of the photodarkening of the 60 nm thick chalcogenide layer. (b) Time dependence of the cavity resonance for 60 and 30 nm  $\text{As}_2\text{S}_3$  during the tuning process.

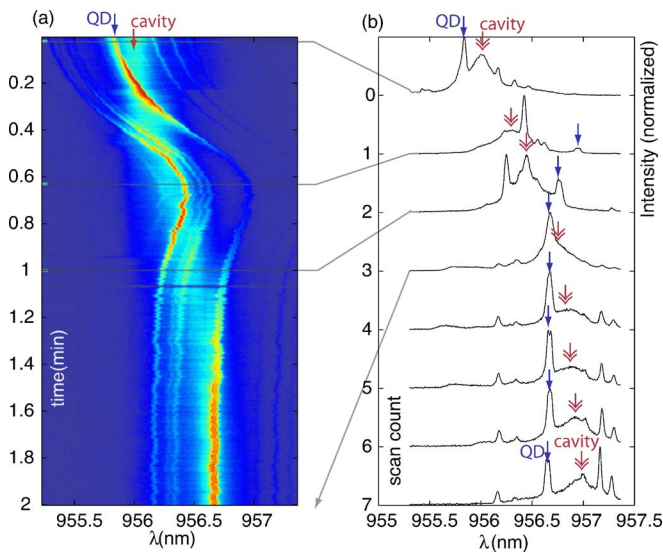


FIG. 3. (Color online) (a) Spectra showing cavity and QD shifting, as a function of exposure time. The QD lines first shift rapidly, presumably through changing material strain induced by the chalcogenide layer. Soon after, the QD lines become stationary, while the cavity continues to redshift. This data set was taken on a sample with 50 nm of  $\text{As}_2\text{S}_3$ . (b) Individual scans of QD/cavity tuning show that after strain relaxation, the cavity can be shifted independently of the QDs. Scans 4–7 were taken for  $t > 2$  min when the pump power was temporarily increased to speed up the chalcogenide exposure.

the compressive pressure exceeds the material's tensile strength.<sup>19</sup> Once the strain is relaxed, only the cavity continues to redshift. In applications where QDs must be tuned independent of the cavity, it might be necessary to first relax the strain or induce fracturing of the chalcogenide layer in some other way. However, we note that this ability to induce local strain may actually be useful for other applications, such as creating locally strained quantum wells,<sup>20</sup> quantum dots, or impurities.<sup>21</sup>

For our experiment, the smallest area that can be locally tuned is a few square microns, limited by the size of the laser beam focus, and the propagation of the structural changes in the glass layer. The locality of the technique allows for independent tuning of interconnected optical components on photonic crystal chips. The method is not only suitable for GaAs devices but can possibly be implemented with any other material, including silicon nanophotonic circuits. Also, the  $\text{As}_2\text{S}_3$  can easily be replaced by other types of chalcogenide glasses or other photosensitive materials depending on the specific application.

In conclusion, we have shown that  $\text{As}_2\text{S}_3$  can be combined with semiconductor photonic crystals to create nanophotonic devices whose optical properties can be independently fine tuned on the same chip. This technique is relevant for fabrication of integrated nanophotonic circuits for classical and quantum information processing, including applications such as filtering, multiplexing, optical storage, fine

tuning of modulators and lasers, and local tuning of distinct PC cavities on GaAs/InAs chips for quantum optics.

Financial support was provided by ONR Young Investigator Award, the MURI Center for photonic quantum information systems (ARO/DTO Program No. DAAD19-03-1-0199), and NSF Grant No. CCF-0507295. Work was performed in part at the Stanford Nanofabrication Facility of NNIN supported by the National Science Foundation under Grant No. ECS-9731293. CUDOS is an Australian Research Council Centre of Excellence.

<sup>1</sup>S. Noda, A. Chutinan, and M. Imada, *Nature (London)* **407**, 608 (2000).

<sup>2</sup>S. Noda, *Lightwave Technol.* **24**, 4554 (2006).

<sup>3</sup>M. F. Yanik and S. Fan, *Phys. Rev. A* **71**, 013803 (2004).

<sup>4</sup>T. Tanabe, K. Nishiguchi, A. Shinya, E. Kuramochi, H. Inokawa, M. Notomi, K. Yamada, T. Tsuchizawa, T. Watanabe, H. Fukuda, H. Shinjima, and S. Itabashi, *Appl. Phys. Lett.* **90**, 031115 (2007).

<sup>5</sup>D. Englund and J. Vuckovic, *Opt. Express* **14**, 3472 (2006).

<sup>6</sup>S. Song, S. S. Howard, Z. Liu, A. O. Dirisu, C. F. Gmachl, and C. B. Arnold, *Appl. Phys. Lett.* **89**, 041115 (2006).

<sup>7</sup>M. W. Lee, C. Grillet, C. L. C. Smith, D. J. Moss, B. J. Eggleton, D. Freeman, B. Luther-Davies, S. Madden, A. Rode, Y. Ruan, and Y. H. Lee, *Opt. Express* **15**, 1277 (2007).

<sup>8</sup>A. Faraon, E. Waks, D. Englund, I. Fushman, and J. Vuckovic, *Appl. Phys. Lett.* **90**, 073102 (2007).

<sup>9</sup>A. Faraon, D. Englund, I. Fushman, J. Vuckovic, N. Stoltz, and P. Petroff, *Appl. Phys. Lett.* **90**, 213110 (2007).

<sup>10</sup>D. Englund, A. Faraon, B. Zhang, Y. Yamamoto, and J. Vučković, *Opt. Express* **15**, 5550 (2007).

<sup>11</sup>K. Hennessy, A. Badolato, A. Tamboli, P. M. Petroff, E. Hu, M. Atatüre, J. Dreiser, and A. Imamoglu, *Appl. Phys. Lett.* **87**, 021108 (2005).

<sup>12</sup>S. Strauf, M. T. Rakher, I. Carmeli, K. Hennessy, C. Meier, A. Badolato, M. J. A. DeDood, P. M. Petroff, E. L. Hu, E. G. Gwinn, and D. Bouwmeester, *Appl. Phys. Lett.* **88**, 043116 (2006).

<sup>13</sup>C. Grillet, C. Monat, C. L. C. Smith, B. J. Eggleton, and D. J. Moss, *Opt. Express* **15**, 1267 (2007).

<sup>14</sup>Y. Akahane, T. Asano, B.-S. Song, and S. Noda, *Nature (London)* **425**, 944 (2003).

<sup>15</sup>D. Englund, D. Fattal, E. Waks, G. Solomon, B. Zhang, T. Nakaoka, Y. Arakawa, Y. Yamamoto, and J. Vučković, *Phys. Rev. Lett.* **95**, 013904 (2005).

<sup>16</sup>A. Schulte, C. Rivero, K. Richardson, K. Turcotte, V. Hamel, A. Ville-neuve, T. Galstain, and R. Vallee, *Opt. Commun.* **1**, 125 (2001).

<sup>17</sup>S. Kugler, J. Hegedus, and K. Kohary, *J. Mater. Sci.: Mater. Electron.* **18**, S163 (2007).

<sup>18</sup>S. J. Skuban, F. Skuban, S. R. Lukic, and Z. Cvejcic, *J. Therm. Anal. Calorim.* **71**, 439 (2003).

<sup>19</sup>We estimate that without fracture, the chalcogenide layer would reach a tensile stress of  $\sigma = Y_m \Delta L / L \approx 0.3$  GPa, where  $Y_m \approx 20$  GPa is Young's modulus, and  $\Delta L / L \approx 0.015$  is the shrinkage.  $\sigma$  exceeds the glass's tensile strength of  $\sim 0.1$  GPa (Refs. 22 and 23), so we expect material fracture. Because of electron charging of the glass layer during scanning electron microscopy, we could not observe fracture lines, but place a bound of less than 15 nm on their width.

<sup>20</sup>J. C. Sturm, H. Manoharan, L. C. Lenchyshyn, M. L. W. Thewalt, N. L. Rowell, J.-P. Noël, and D. C. Houghton, *Phys. Rev. Lett.* **66**, 1362 (1991).

<sup>21</sup>C. Santori, P. Tamarat, P. Neumann, J. Wrachtrup, D. Fattal, R. G. Beausoleil, J. Rabeau, P. Olivero, A. D. Greentree, S. Praver, F. Jelezko, and P. Hemmer, *Phys. Rev. Lett.* **97**, 247401 (2006).

<sup>22</sup>VITRON Spezialwerkstoffe, see ([http://cvdmaterials.de/chalcogenide\\_glasses.htm](http://cvdmaterials.de/chalcogenide_glasses.htm)), 2007.

<sup>23</sup>V. F. Chuprakov, V. V. Sakharov, N. M. Kononova, E. N. Loitsker, G. E. Kharitonova, and I. A. Baryshnikov, *Glass Ceram.* **48**, 5 (1991).